Article:
Schulte-Braucks, C, Glass, S, Hofmann, E et al. (2017) Process Modules for GeSn Nanoelectronics with high Sn-contents. Solid-State Electronics, 128. pp. 54-59. ISSN: 0038-1101

https://doi.org/10.1016/j.sse.2016.10.024

Process Modules for GeSn Nanoelectronics with high Sn-contents

C. Schulte-Braucks, S. Glass, E. Hofmann, D. Stange, N. von den Driesch, J.M. Hartmann, Z. Ikonic, Q.T. Zhao, D. Buca, S. Mantl

PII: S0038-1101(16)30189-7
DOI: http://dx.doi.org/10.1016/j.sse.2016.10.024
Reference: SSE 7121

To appear in: *Solid-State Electronics*

Please cite this article as: Schulte-Braucks, C., Glass, S., Hofmann, E., Stange, D., von den Driesch, N., Hartmann, J.M., Ikonic, Z., Zhao, Q.T., Buca, D., Mantl, S., Process Modules for GeSn Nanoelectronics with high Sn-contents, *Solid-State Electronics* (2016), doi: http://dx.doi.org/10.1016/j.sse.2016.10.024

Process Modules for GeSn Nanoelectronics with high Sn-contents

C.Schulte-Braucks[1], S. Glass[1], E. Hofmann[1], D. Stange[1], N. von den Driesch[1], J.M. Hartmann[2], Z. Ikonic[3], Q.T. Zhao[1], D. Buca[1], S. Mantl[1]

[1]Peter-Gruenberg-Institute 9 (PGI-9) and JARA-FIT, Forschungszentrum Juelich GmbH, 52428 Juelich, Germany

[2]University of Grenobles Alpes, F38000 and CEA, LETI, MINATEC Campus, F-38054, Grenoble, France

[3]Institute of Microwaves and Photonics, School of Electronic and Electrical Engineering, University of Leeds, LS2 9JT, Leeds, United Kingdom

Abstract - This paper systematically studies GeSn n-FETs, from individual process modules to a complete device. High-k gate stacks and NiGeSn metallic contacts for source and drain are characterized in independent experiments. To study both direct and indirect bandgap semiconductors, a range of 0 at.% to 14.5 at.% Sn-content GeSn alloys are investigated. Special emphasis is placed on capacitance-voltage (C-V) characteristics and Schottky-barrier optimization. GeSn n-FET devices are presented including temperature dependent I-V characteristics. Finally, as an important step towards implementing GeSn in tunnel-FETs, negative differential resistance in $Ge_{0.87}Sn_{0.13}$ tunnel-diodes is demonstrated at cryogenic temperatures. The present work provides a base for further optimization of GeSn FETs and novel tunnel FET devices.

Keywords—GeSn, MOSFET, high-k/metal gate, NiGeSn

I. INTRODUCTION

Recently, GeSn alloys have emerged as promising group IV semiconductors for electronic [1] as well as photonic [2], [3] applications. The breakthrough in epitaxial growth of high-Sn content and strain relaxed layers, enabled fundamental direct bandgap group IV alloys grown on Si [4,5]. The direct bandgap property is a requirement for efficient Si based light emitters. However, such alloys may also serve as performance boosters in nanoelectronics. The small effective mass and associated reduction of intra-valley scattering yields high mobility Γ-electrons. Performance of GeSn based n-type Metal Oxide Semiconductor Field Effect Transistors (MOSFETs) should then be superior to those of their pure Ge counterparts. In addition, the possibility of combining direct band-to-band tunneling and low bandgap should yield efficient tunnel field effect transistors (TFETs).

Mobility calculations, using the 8-band k.p method for the Γ-valley band structure and effective mass (including nonparabolicity) for the L-valley band structure, predict a significant mobility enhancement as soon as the population of Γ-valley is sufficiently large. The calculations take acoustic phonon, deformation potential, alloy disorder, ionized impurity, and inter-valley scattering into account. Modulation of the Γ-valley population can be achieved either by changing Sn-content or layer strain. For Sn contents below ~9 at.% GeSn alloys are indirect bandgap semiconductors. Hence, the electron mobility is dominated by electrons occupying the L-valley. For larger Sn contents, above the indirect to direct bandgap transition, the Γ-valley becomes increasingly populated and the electron mobility is boosted significantly. The calculated Sn-dependent Γ-valley population and effective (weighted-average) mobility is shown in Fig.1(a). GeSn pseudomorphically grown on Ge is Sn-content dependently biaxially compressively strained. However, growing thicker GeSn layers leads to strain relaxation or even tensilely strained GeSn when combining different Sn-contents [6,7]. Decreasing compressive strain has the same effect as increasing Sn content, leading to an increase of Γ-valley population and of Γ-electron mobility according to Fig.1 (b). In contrast, L-electron mobility is of the order of $4x10^3$ cm^2/Vs for all Sn-contents and strain values presented here. The

large difference between Γ- and L-electron mobility comes from a much larger effective mass of the L-electrons. However, just above the indirect to direct transition, the Γ-electron mobility is still limited by strong inter-valley Γ-L scattering, which gives a large relative contribution to total scattering due to a large L-valley density of states (while the L-electrons are less affected, because of a smaller density of states of Γ). Together with a small fraction of Γ-electrons, this implies that in alloys with 8.5 at.% Sn, at the direct to indirect transition, the mobility is always dominated by the L-electrons. However, when Γ-L spacing increases, by decreasing strain or increasing Sn-content, inter-valley scattering is reduced, and Γ-population becomes significant. Consequently, not only the Γ-electron mobility but also the effective electron mobility, displayed in Fig.1(c), strongly increases. It is also worth noting that biaxial strain induces a non-negligible anisotropy of the Γ-valley, and in case of compressive strain the in-plane mobility, relevant for MOSFETs, is larger (by up to ~20%) than perpendicular mobility.

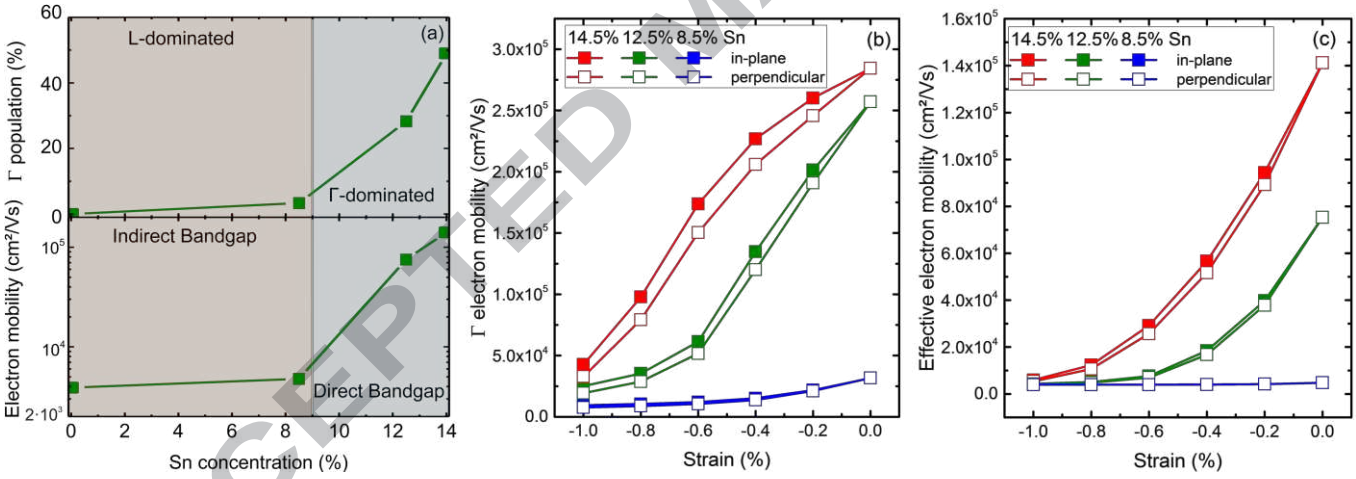

Fig. 1: (a) Calculated Γ-valley population (top) and effective electron mobility, at 300K and 10^{14} cm^{-3} electron density, vs Sn-content (bottom) at zero strain. (b) Γ and (c) effective electron mobilities for various GeSn alloys, dependent on biaxial strain.

Preliminary works on p- and n- MOSFETs [8], [9] and even TFETs [10] based on GeSn alloys have been reported, however, the Sn-contents and strain values were far below the indirect to direct transition. The low solid solubility of Sn in Ge < 1 at.% and the non-equilibrium growth restricts the thermal budget to temperatures < 350°C for Sn-contents above 10 at.% making process integration challenging.

In this work we discuss advances on low temperature process modules for GeSn-FET devices with Sn-contents up to 13 at.%, including high-k/metal gate stack deposition and low resistivity metallic NiGeSn contact formation. Emphasis is placed on the fabrication and characterization of metal-semiconductor-metal (MSM) diodes for Schottky-barrier height (SBH) extraction and Schottky-barrier tuning by dopant segregation (DS). GeSn n-FETs are fabricated using these modules and, as a step towards novel devices, *p-i-n* tunneling diode characterization is presented.

II. EXPERIMENTAL

Due to the low solid solubility of Sn in Ge (< 1 at.%) growth conditions for GeSn with up to 13 at.% Sn are far from equilibrium. An industry compatible AIXTRON TRICENT RP-CVD epitaxial reactor was employed to grow these layers on 200 mm Ge buffered Si(100) wafers [11]. All process temperatures were kept below 350°C in order to avoid Sn-diffusion and segregation. As a first key module, MOS-capacitors (MOScaps) with high-k/metal gate stacks on GeSn were investigated. After a wet HF-HCl surface preparation, 6 nm HfO_2 high-k dielectric was deposited at low temperature by atomic layer deposition (ALD) followed by 40 nm sputter deposited TiN metallization both using 200 mm, industry compatible reactors. MOScaps with Sn-contents between 0 at.% (Ge-substrate) and 12.5 at.% were fabricated. Standard CMOS technology, such as photo lithography and reactive ion etching, was used to define the structures. The fabrication ended with a lift-off process after the deposition of 150 nm Al for contacts followed by forming gas annealing at 300°C. A set of Capacitance-Voltage (C-V) characteristics at different frequencies measured on $TiN/HfO_2/Ge_{0.915}Sn_{0.085}$ capacitors is shown in Fig. 2(a). The good $GeSn/HfO_2$ interface quality is evidenced by the small frequency dependent flat-band voltage shift and the small frequency dispersion in accumulation. Typical for low bandgap semiconductors, the C-V curves feature a strong minority carrier inversion response even at high frequencies > 100 kHz. As a consequence, a reliable extraction of the interface state density (Dit) using the conduction method at *room temperature* becomes difficult [12]. However, the minority carrier inversion response is reduced at lower temperatures. We have thus used the

low temperature conductance method as described in work by Nicollian and Brews[13] at T<120 K to extract Dit values of $2x10^{12}$ $cm^{-2}eV^{-1}$ at midgap for GeSn capacitors with different Sn contents (Fig. 2(b)). A study focusing on the process development and characterization of ternary SiGeSn MOScaps has been published recently [14].

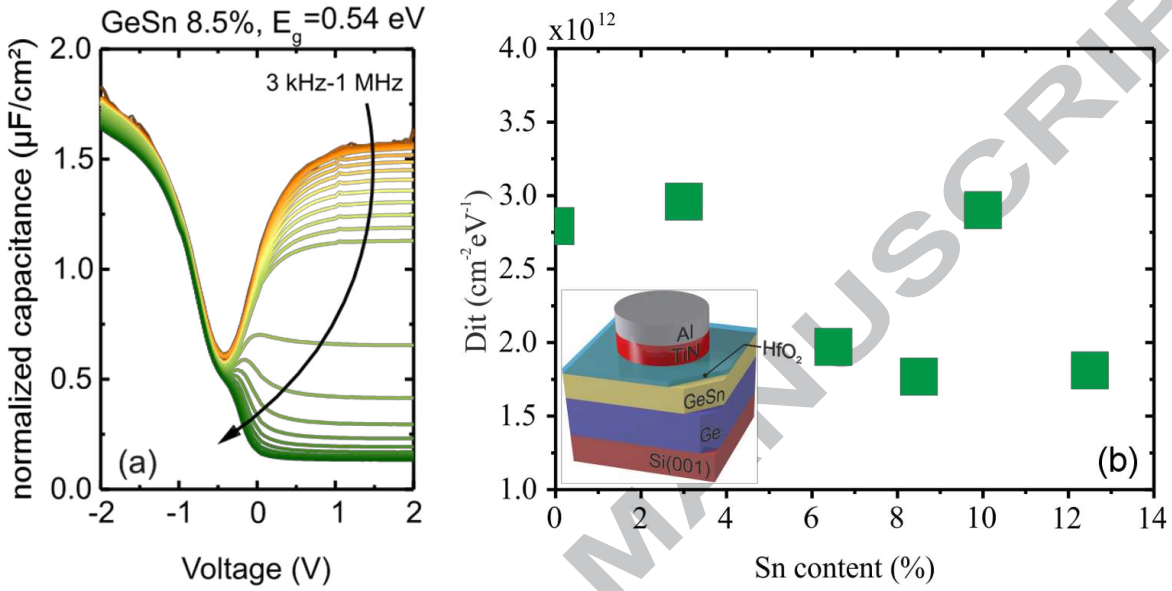

Fig. 1: (a) CV-characteristics of TiN/6 nm HfO2/Ge0.915Sn0.085 MOScap for a set of frequencies. (b) Dit at midgap for several Sn-contents extracted at temperatures below 120 K.

A second fundamental module is contact formation. Metal-semiconductor-metal (MSM) diodes based on NiGeSn/GeSn Schottky contacts were fabricated using an oxide mask. After native oxide removal, 10 nm of Ni were deposited by sputter deposition and ~ 23 nm NiGeSn was formed by rapid thermal annealing for 10 s in N_2/H_2 forming gas atmosphere. Unreacted Ni was removed by sulfuric acid (96 % aq.). The van-der-Pauw method[15] has been used to measure the sheet resistance of the so formed NiGeSn films. The lowest sheet resistance was obtained by stano-germanidation at 325°C [16]. The low-resistive NiGeSn-phase could be maintained over the complete available Sn-content range from 0 to 12.5 at.%. The sheet resistance of NiGeSn for several Sn-contents is shown in Fig.3(d). Furthermore, a smooth NiGeSn/GeSn interface was obtained as shown by the cross-sectional Transmission-Electron-Microscopy (TEM) image in the inset of Fig.3(d).

Current transport properties across a metal-semiconductor contact are determined by the Schottky-barrier. Previous studies have investigated the electron Schottky-barrier on NiGeSn/$Ge_{0.958}Sn_{0.042}$ [17] and hole Schottky-barrier on NiGeSiSn/$Ge_{0.86}Si_{0.07}Sn_{0.07}$ [18]. Here, we determine the NiGeSn/GeSn hole Schottky-barrier from MSM diodes with different contact areas and for several Sn-concentrations using the activation-energy method. The advantage of this method is that the electrically active contact area does not need to be known, e.g. current crowding does not affect the Schottky-barrier extraction. The temperature dependent I-V characteristics were measured in a liquid nitrogen cooled cryostat under high vacuum where the temperature range from 400 K to 100 K is covered in 10 K incremental steps. From Arrhenius plots of the current characteristics for different voltages (Fig. 3(a)) the Schottky-barrier height (SBH) was extracted. According to thermionic-emission-diffusion theory, the voltage dependent SBH can be extracted from the slope *s* of the linear region in the $\ln|I/T^2|$ plot via

$$\mathrm{SBH} = -s \cdot \frac{k}{e},$$

where *k* is Bolzmann's constant and *e* the electron charge. Outside this linear region, the current is determined by the series resistance (high temperatures) or the shunt resistance (low temperatures). The primary source of the former is the GeSn resistivity while the latter is impacted by parasitic currents. As the MSM diode consists of two back-to-back Schottky diodes, the current corresponds to the reverse bias I-V characteristic at all times. The magnitude of the current is given by the lower Schottky-barrier – hole or electron barrier – in undoped semiconductors. In our case the hole Schottky-barrier is observed, as the nominally intrinsic GeSn layers are actually p-type. The main reasons for the voltage dependence of the SBH observed in Fig. 3(b) are image force and static lowering due to the applied voltage. By linearly extrapolating to 0 V these effects are suppressed and the hole Schottky-barrier is obtained. Fig. 3(c) shows the results for NiGeSn/GeSn Schottky contacts with Sn contents of 0 at.%, 7 at.% and 12.5 at.%. Throughout the entire Sn content range, the hole Schottky-barrier remains below 0.10 eV, making NiGeSn an ideal contact for p-type

devices. However, this might imply very high Schottky-barriers for electrons leading to high S/D resistances for n-type GeSn and demanding further investigation on n-type GeSn-contacts over a wide Sn-content range.

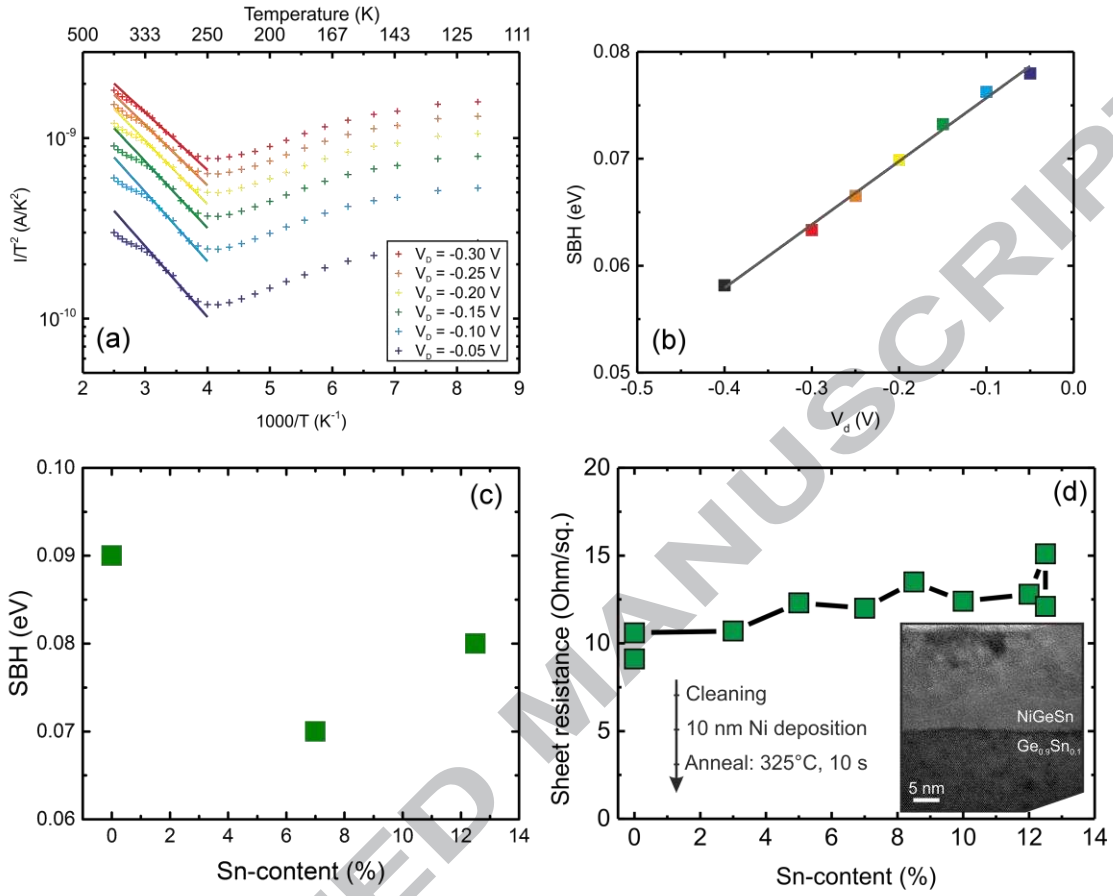

Fig. 3: Investigation of NiGeSn Schottky-contacts. (a) Arrhenius plot of current characteristics for a 12.5 at.% Sn sample. The linear region is fitted and SBH is extracted from the slope. (b) SBH vs. applied bias from (a). The SBH for 0 V is extracted by linear extrapolation. (c) Extracted 0 V SBH for various Sn contents. (d) Sheet resistance of NiGeSn fabricated on several GeSn layers. The inset depicts a TEM micrograph of a NiGeSn/GeSn contact.

For a metal-semiconductor interface with high carrier concentrations, the tunneling current component through the barrier is increased, which reduces the experimentally observed SBH. A well-known method to modify the SBH using this effect is dopant segregation [19]. Dopants are implanted shallowly into the contact windows before metallization. During the following stano-germanidation step the entire implanted region is consumed. Therefore, semiconductor quality is conserved as the damaged area is fully converted to stano-germanide. The high-crystalline quality can be seen in the high-resolution TEM-image in Fig.4.

Fig. 4: High-resolution TEM image of the NiGeSn/GeSn interface after BF_2 implantation with 10 kV and $1x10^{15}cm^{-2}$ proving the good crystalline quality of the GeSn after NiGeSn-formation

Due to the different solubility of dopants in metal and semiconductor the snow plough effect leads to dopant diffusion through the metallic region into the semiconductor at the interface. This results in a sharp doping profile with a high dopant concentration at the metal-semiconductor interface. The dopant segregation effect in GeSn for both n- and p-type dopants is presented below. Phosphorous (P), arsenic (As) and boron (BF_2) were implanted into GeSn test-structures with a dose of $1x10^{15}$ cm^{-2} at energies of 7, 13 and 10 keV, respectively. In GeSn, P and As act as n-type dopants, while B is a p-type dopant. The implanted region was then converted into NiGeSn as described above. Subsequently, doping profiles were measured by means of Time of Flight Secondary-Ion-Mass-Spectrometry (ToF-SIMS). Whereas there is no peak visible in the doping profile for P, a snow plough effect is observed for both As and B leading to a peak in the As/B-concentration at the NiGeSn/GeSn interface (Fig. 5). The differences in DS for the n-type dopants As and P might be attributed to differences in solubility and diffusion. Nonetheless, as DS is possible both for n- and p-type dopants, this effect can be used to modify the SBH.

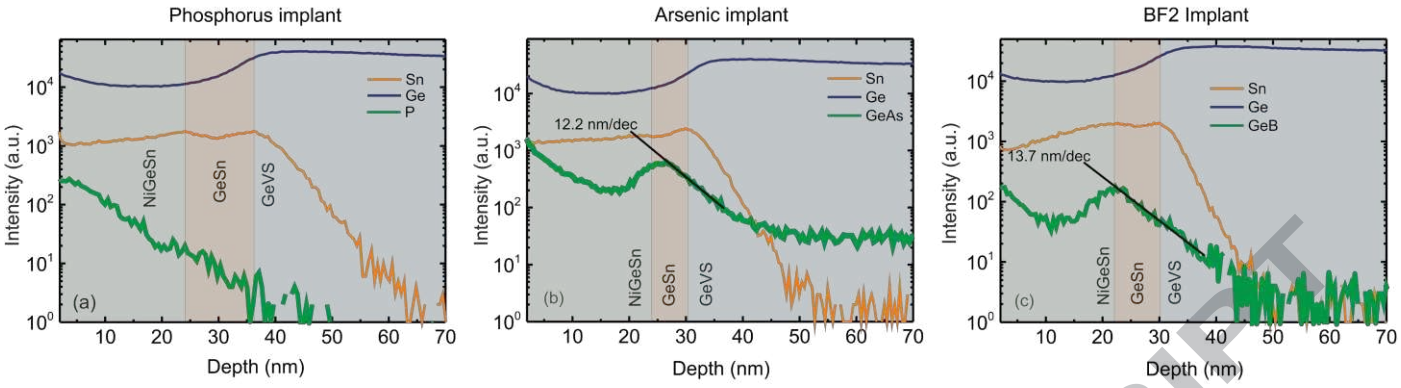

Fig. 5: SIMS-profiles of NiGeSn/GeSn contacts with 10 at.% Sn: For Phosphorous impantation no segregation was observed (a), whereas there is a clear peak in the Arsenic (b) and Boron (c) profiles. For higher sensitivity As and B are measured as GeAs and GeB.

In order to investigate the impact of DS, NiGeSn contacts were fabricated on in-situ phosphorus doped $Ge_{0.875}Sn_{0.125}$ (GeSn:P) with a $2.7x10^{18}$ cm^{-3} n-type carrier concentration. DS was then performed with As or B using the process described above. Since activated As provides electrons in GeSn, DS increases the majority carrier concentration at the NiGeSn/GeSn:P interface. For p-type B, DS yields the opposite. An increase in majority carrier concentration at the interface allows for a higher tunneling component through the barrier. Consequently, the effective SBH observed by the charge carriers is reduced. Fig. 6 shows I-V characteristics measured from one NiGeSn contact to the next, for samples without DS or with As or B DS. As expected, the I-V curves become more and more Ohmic when increasing the electron concentration at the NiGeSn/GeSn:P interface (e.g. by switching from B DS to no DS to As DS samples).

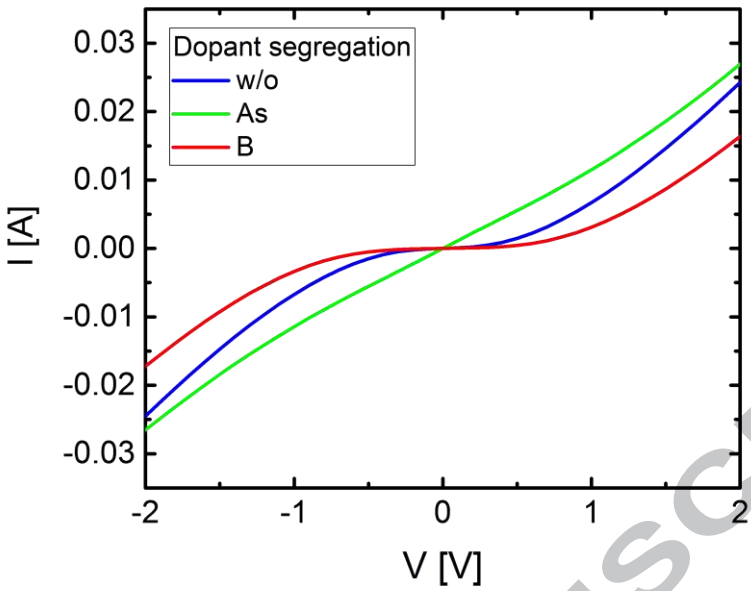

Fig. 6: Impact of DS on n-type Ge0.875Sn0.125:P. As the n-type carrier concentration at the NiGeSn/GeSn:P interface increases, the I-V characteristic becomes more Ohmic.

Combining the above described process modules, GeSn n-MOSFETs were fabricated with Sn-contents of 0 at.%, 7 at.% and 12.5 at.% using ion implanted source/drain (S/D) contacts after forming a gate stack with TiN/HfO_2. Transfer curves of $Ge_{0.93}Sn_{0.07}$ n-FETs for a series of temperatures are shown in Fig. 7.

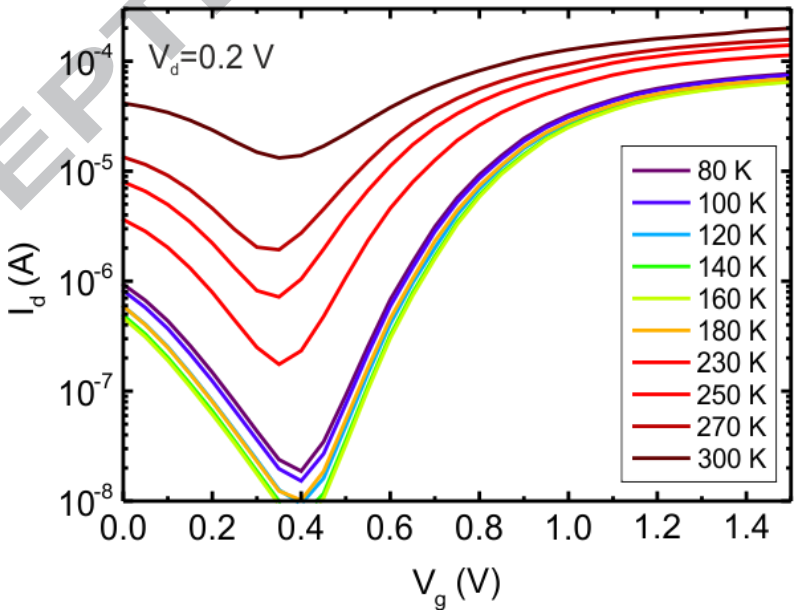

Fig. 7: Transfer characteristics of Ge0.93Sn0.07 n-FETs at different temperatures.

At room temperature, the device shows a low I_{on}/I_{off} ratio while a reduced on current at lower temperatures is due to the poor n+/p junctions in the S/D regions. The limited process temperatures used here in order to avoid Sn diffusion (max. 300°C), was not enough to recrystallize the amorphized regions created by ion implantation, leading to very poor junctions with low activation and high access resistances. This is even more critical for high Sn-content devices, as shown in Fig. 8 at 80 K. Apart from the un-healed implantation damage, the unintentional background doping of GeSn increases with the Sn-content. Furthermore, the bandgap is decreased. Both factors lead to increased S/D-leakage and gate induced drain-leakage (GIDL) which is caused by band-to-band tunneling and increases exponentially with the reduced bandgap. This is also visible in the temperature dependence of the transfer characteristics in Fig. 7. The S/D leakage strongly decreases for temperatures below 200 K. The solution for maintaining crystalline GeSn is the use of in-situ doping and selective growth in the S/D region. The in-situ doping is discussed below in terms of tunneling diodes.

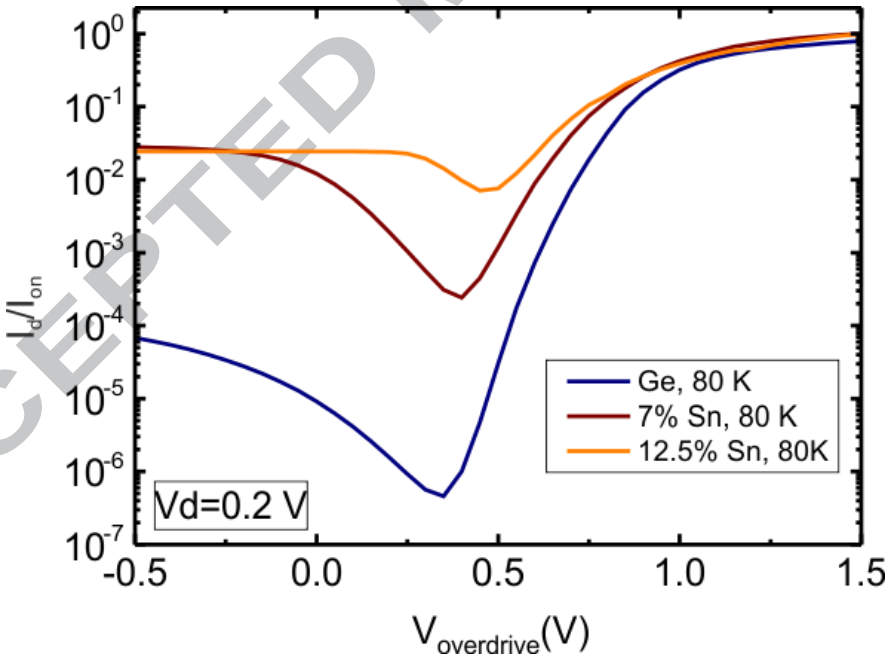

Fig. 8: I_d/I_{on} ratio of GeSn n-FETs at 80 K for several Sn-contents.

As a demonstration of the potential of direct bandgap GeSn for band to band tunneling and the advantage of in-situ doping over ion implantation, we have fabricated GeSn tunneling diodes as an important step

towards advanced GeSn based TFETs. We could push the Sn-content up to 13 at.% as a follow up to previous results with a stack of 9 at.% and 11 at.% [1] enabling an even lower bandgap and higher directness of the GeSn. As a proof of band-to-band tunneling, negative differential resistance (NDR) is observed at cryogenic temperatures (Fig. 9), demonstrating a high doping level of both p- and n-type dopants, which is essential for MOSFETs and TFETs. However, due to enhanced diffusion and trap assisted tunneling (TAT) in this low-bandgap semiconductor, the NDR vanishes for temperatures above 100 K. For forward bias > 0.1 V two distinct regions, separated by a kink in the slope of the I-V curve, are visible. While the middle part of the curve 0.1 V < V_d < 0.3 V can be attributed to TAT, the diffusion current dominates for strong forward bias > 0.3 V. We expect further improvements in the peak to valley current ratio and a move towards room temperature NDR with optimized doping profiles.

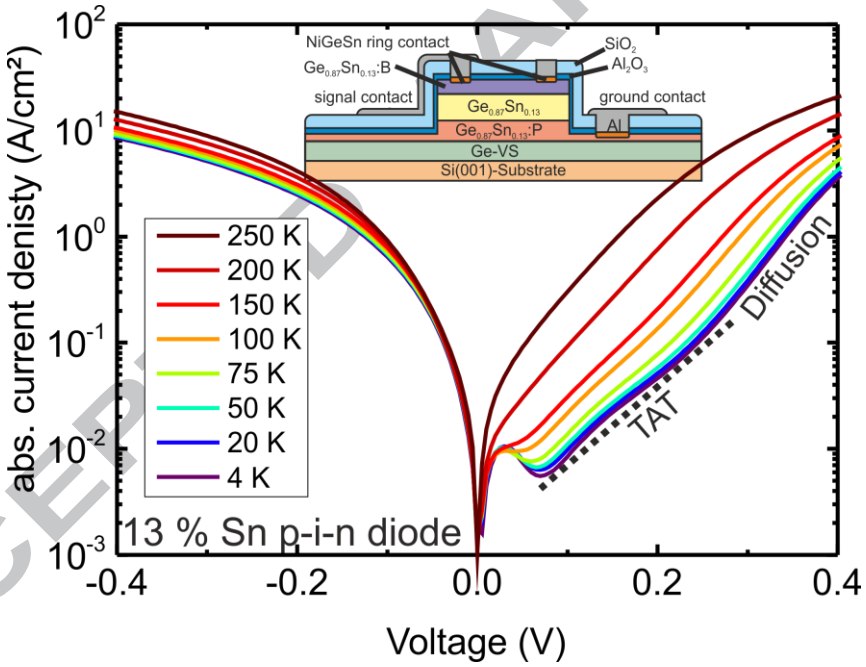

Fig. 9: Temperature dependent I-V measurements of a Ge0.87Sn0.13 p-i-n diode showing clear NDR at cryogenic temperatures.

III. CONCLUSION

In this work, process module developments for GeSn FETs were presented and assembled to for the fabrication of GeSn n-FETs. A wide range of Sn-contents was covered, allowing the study of both indirect

and direct bandgap GeSn alloys. TiN/HfO_2/GeSn MOScaps, showing good C-V characteristics with Dit levels of 10^{12} $eV^{-1}cm^{-2}$, have been studied for use as gate stacks. NiGeSn is shown to have low sheet resistances over the entire Sn-content range and very small Schottky barrier heights on p-GeSn. To further optimize the Schottky contacts, dopant segregation with both As and B, was demonstrated for NiGeSn contacts. In the case of n-GeSn, it is shown that As dopant segregation leads to increasingly Ohmic contact behavior. Due to the metastability of GeSn, junctions made by ion implantation have proven to be challenging. A possible solution is in-situ doping which reveals its potential in GeSn-tunnel diodes with 13 at.% Sn where characteristic negative differential resistance is observed at cryogenic temperatures.

IV. ACKNOWLEDGMENTS

This research received funding from the EU FP7 project E2SWITCH (619509) and the BMBF project UltraLowPow (16ES0060 K)

REFERENCES

[1] Schulte-Braucks C, Stange D, von den Driesch N, Blaeser S, Ikonic Z, Hartmann JM, et al. Negative differential resistance in direct bandgap GeSn p-i-n structures. Appl Phys Lett 2015;107:042101–1 – 4. doi:10.1063/1.4927622.

[2] Soref RA, Buca D, Yu S-Q. Group IV Photonics- Driving Integrated Optoelectronics. Opt Photonics News 2016;January:32–9.

[3] Wirths S, Geiger R, Driesch NV Den, Stange D, Zabel T, Ikonic Z, et al. Direct Bandgap GeSn Microdisk Lasers at 2 . 5 μm for Monolithic Integration on Si-Platform, 2015, p. 36–9.

[4] Wirths S, Geiger R, Driesch NV Den, Mussler G, Stoica T, Mantl S, et al. Lasing in direct-bandgap GeSn alloy grown on Si 2015:1–14. doi:10.1038/nphoton.2014.321.

[5] Stange D, Wirths S, von den Driesch N, Mussler G, Stoica T, Ikonic Z, et al. Optical Transitions in

Direct-Bandgap $Ge_{1-x}Sn_x$ Alloys. ACS Photonics 2015;2:1539–45. doi:10.1021/acsphotonics.5b00372.

[6] Wirths S, Ikonic Z, Tiedemann AT, Holländer B, Stoica T, Mussler G, et al. Tensely strained GeSn alloys as optical gain media. Appl Phys Lett 2013;103:192110_1–192110_5. doi:10.1063/1.4829360.

[7] Wirths S, Stange D, Pampillón M-A, Tiedemann AT, Mussler G, Fox A, et al. High- k Gate Stacks on Low Bandgap Tensile Strained Ge and GeSn Alloys for Field-Effect Transistors. ACS Appl Mater Interfaces 2015;7:62–7. doi:10.1021/am5075248.

[8] Gupta S, Vincent B, Yang B, Lin D, Gencarelli F, Lin J-YJ, et al. Towards high mobility GeSn channel nMOSFETs: Improved surface passivation using novel ozone oxidation method. IEDM 2012:16.2.1–16.2.4. doi:10.1109/IEDM.2012.6479052.

[9] Han G, Su S, Zhan C, Zhou Q, Yang Y, Wang L, et al. High-Mobility Germanium-Tin (GeSn) P-channel MOSFETs Featuring Metallic Source / Drain and Sub-370 ° C Process Modules 2011:402–4.

[10] Yang Y, Su S, Guo P, Wang W, Gong X, Wang L, et al. Towards direct band-to-band tunneling in P-channel tunneling field effect transistor (TFET): Technology enablement by Germanium-tin (GeSn). 2012 Int Electron Devices Meet 2012:16.3.1–16.3.4. doi:10.1109/IEDM.2012.6479053.

[11] von den Driesch N, Stange D, Wirths S, Mussler G, Holländer B, Ikonic Z, et al. Direct Bandgap Group IV Epitaxy on Si for Laser Applications. Chem Mater 2015;27:4693–702. doi:10.1021/acs.chemmater.5b01327.

[12] Martens K, Chui CO, Brammertz G, De Jaeger B, Kuzum D, Meuris M, et al. On the Correct Extraction of Interface Trap Density of MOS Devices With High-Mobility Semiconductor Substrates. IEEE Trans Electron Devices 2008;55:547–56. doi:10.1109/TED.2007.912365.

[13] Nicollian EH, Brews JR. MOS (Metal Oxide Semiconductor) Physics and Technology. Wiley; 2002.

[14] Schulte-Braucks C, von den Driesch N, Glass S, Tiedemann AT, Breuer U, Besmehn A, et al. Low

Temperature Deposition of High-k/Metal Gate Stacks on High-Sn Content (Si)GeSn-Alloys. ACS Appl Mater Interfaces 2016:acsami.6b02425. doi:10.1021/acsami.6b02425.

[15] van der Pauw LJ. A method of measuring the resistivity and hall coefficient of discs of arbitrary shape. Philips Res Reports 1958;13:1–9. doi:citeulike-article-id:8438442.

[16] Wirths S, Troitsch R, Mussler G, Hartmann J-M, Zaumseil P, Schroeder T, et al. Ternary and quaternary Ni(Si)Ge(Sn) contact formation for highly strained Ge p- and n-MOSFETs. Semicond Sci Technol 2015;30:055003–1 – 8. doi:10.1088/0268-1242/30/5/055003.

[17] Tong Y, Han G, Liu B, Yang Y, Wang L, Wang W, et al. Ni (Ge 1 − x Sn x) Ohmic Contact Formation on N-Type Ge 1 − x Sn x Using Selenium or Sulfur Implant and Segregation. IEEE Trans Electron Devices 2012;60:1–7.

[18] Zheng J, Wang S, Zhang X, Liu Z, Xue C, Li C. Ni(Ge1-x-ySixSny) Ohmic Contatct Formation on p-type Ge0.86Si0.07Sn0.07. IEEE Electron Device Lett 2015;36:878–80. doi:10.1109/LED.2015.2459062.

[19] Mueller M, Zhao QT, Urban C, Sandow C, Buca D, Lenk S, et al. Schottky-barrier height tuning of NiGe/n-Ge contacts using As and P segregation. Mater Sci Eng B 2008;154-155:168–71. doi:10.1016/j.mseb.2008.09.037.